Transportation Research Part D 101 (2021) 103090

Contents lists available at ScienceDirect

Transportation Research Part D

journal homepage: www.elsevier.com/locate/trd

Empirical investigation of the emission-macroscopic fundamental diagram

Emmanouil Barmpounakis [a,*,1], Martí Montesinos-Ferrer [a,1], Eric J. Gonzales [b], Nikolas Geroliminis [a]

[a] École Polytechnique Fédérale de Lausanne (EPFL), Station 18, CH-1015 Lausanne, Switzerland
[b] University of Massachusetts Amherst, MA 01003-0724, Amherst, MA, USA

ARTICLE INFO

Keywords:
Drone dataset
Emissions
Traffic
Congestion

ABSTRACT

Vehicle emissions are a major contributor of air pollution in urban areas, with severe consequences for public health and the environment. This paper focuses on analyzing vehicle emissions in a multimodal urban context to better understand its determinants and investigate relations between emissions and congestion patterns. Thousands of naturalistic trajectories collected with a swarm of drones during the pNEUMA experiment are analyzed and EPA's microscopic emission model, project level MOVES, is implemented to estimate vehicular emissions. The method is developed and illustrated with a CO_2 analysis. The results empirically show the aggregated relationships between congestion and vehicular emissions, while accounting for the individual characteristics of each trajectory. These systematic relationships on a network scale with the use of empirical data, allow us to extend the macroscopic fundamental diagram (MFD) to the emissions-MFD (e-MFD). The spatiotemporal distribution of emissions is also studied, highlighting areas with high concentration over the urban area.

1. Introduction

Road transportation is a major source of air pollutant emissions. It is estimated that the on-road vehicles account for more than half of dangerous air pollutant emissions and over 30% of carbon dioxide emission in the United States (Alson et al., 2014). Globally, 1.3 billion on-road vehicles consume 79 quadrillion British thermal units (BTU) of energy, mostly gasoline and diesel fuels, emit 5.7 gigatonnes of CO_2, and emit other pollutants contributing to approximately 200,000 annual premature deaths (Frey, 2018). Reducing these emissions is important for protecting and improving human health as well as for reducing the production of greenhouse gases, which are associated with global climate change. Emissions from vehicles in traffic play an increasingly important role in urban policy making and traffic management in large metropolitan road networks.

Since accurate measurements in real networks are difficult to obtain, empirical estimation and models are needed to relate these quantities to the vehicle operations in the road network in order to adequately account for the impacts of traffic management policies on emissions of greenhouse gases and other pollutants. Existing models for vehicular emissions generally fall into two main categories: microscopic models that focus on specific movements of individual vehicles and macroscopic models that are based on aggregated data

* Corresponding author.
E-mail address: manos.barmpounakis@epfl.ch (E. Barmpounakis).
[1] Shared first co-authorship (alphabetical order).

https://doi.org/10.1016/j.trd.2021.103090

Available online 27 October 2021

and average values.

A challenge for modeling network traffic emissions is that existing macroscopic emissions models are coarsely related to vehicle operations, typically assigning an emission rate per aggregate vehicle distance traveled based on an assumed driving cycle (Agency, 2003; EMFAC2007, 2007; Ntziachristos et al., 2009). In contrast, the most sophisticated vehicle emission models are based on detailed second-by-second vehicle trajectories, which are not typically observed across a network (Barth et al., 2000; EPA US, 2012; Hausberger, 2003; Rakha et al., 2007). At the same time, understanding network-wide traffic through the macroscopic fundamental diagram (MFD) can optimally allocate demand to existing networks (Geroliminis and Daganzo, 2008). With the recent advances in data acquisition and data management tools, new ways have been unlocked on how traffic and emissions can be monitored, studied, and modeled. In particular, the pNEUMA dataset (Barmpounakis and Geroliminis, 2020), utilizing a swarm of drones over the central district of Athens, Greece, offers a unique opportunity to study the emissions at urban scale with comprehensive observations of close to half a million of detailed vehicle trajectories.

This paper presents a new generation of studies on vehicular emissions in networks by using massive multimodal empirical data with high-resolution at an urban scale. It offers a unique way to further scrutiny the relationships between traffic operations, congestion dynamics, and vehicular emissions, which until now were only explored through microsimulation (Saedi et al., 2020; Shabihkhani and Gonzales, 2014). In particular, it sheds light on the relationships between vehicle operations and corresponding emissions in a network, including how congestion increases emissions, the spatial distribution of emissions in an urban environment and their dynamics over time. The contributions are twofold: i) we provide a method to estimate network-wide emissions by linking naturalistic vehicle trajectory data with microscopic emissions models; and ii) we extend the macroscopic fundamental diagram (MFD) to the emissions-MFD (e-MFD) by providing a set of traffic and emissions empirical data that support analysis of systematic relationships on a network scale.

The paper is organized as follows: Section 2 provides a review of literature on emissions models for vehicles and traffic in networks. Section 3 includes a short description of the pNEUMA dataset, and the underlying microscopic model MOVES. Section 4 analyzes the results both at microscopic and macroscopic level. Finally, conclusions are discussed in Section 5.

2. Literature review

Models for vehicular emissions range from very detailed microscopic models to aggregated regional models. The appropriate model depends on the availability of data and application. For example, pollutants like particulate matter have a very localized impact and are most meaningfully tracked at the individual vehicle and facility level. Greenhouse gases have a global impact, so the aggregate emissions are of interest, although the accuracy of aggregate estimates depends on the sum of individual vehicle operations. It is useful to classify vehicular emissions models by level of detail with microscopic and macroscopic emissions models lying at the ends of a spectrum with various mesoscopic models in between.

Microscopic models are the most detailed models that provide instantaneous emissions estimates based on a vehicle's characteristics and operating conditions. These include "Modal" models, which require second-by-second vehicle speed, acceleration, and/or calculated engine power demand (Frey et al., 2008). Examples include VT-Micro (Rakha et al., 2007), CMEM (Barth et al., 2000), MIT, PHEM (Hausberger, 2003), VERSIT+ (Smit et al., 2007), the project level of MOVES (EPA US, 2012), and CRUISE ("AVL cruise – vehicle system and driveline analysis," 2017). The emission factors for these models are based on detailed look-up tables or regressions that relate direct tailpipe emission measurements with second-by-second inputs. Many of the most recent developments in vehicle emission modeling are developments of microscopic models using PHEM (Lejri et al., 2018), CMEM (Kumar Pathak et al., 2016; Sun et al., 2015), MOVES (Perugu, 2019), and other models (Int Panis et al., 2006; Nyhan et al., 2016; Osorio and Nanduri, 2015). There is general agreement that microscopic models are necessary to capture the underlying mechanism of vehicular emissions and provide accurate estimates. Nevertheless, these models have intense data needs that cannot be easily met for network level approaches, as these data are not available at large scales. Simulated data can be an alternative, but the realism is questionable given that they contain a large number of parameters and assumptions.

Macroscopic emissions models provide a simplified alternative to detailed microscopic models for networks and larger regions. These models use aggregated traffic variables such as average speed, total number of vehicles, and vehicle kilometers traveled to make emissions estimates. Examples include COPERT (Ntziachristos et al., 2009), EMFAC (CARB, 2015), county level of MOVES (EPA US, 2012), and HBEFA (Keller et al., 2017). Although these models utilize relatively few data inputs, making them much easier to implement for large urban networks, they are also insensitive to variations in the cycles of acceleration, cruising, deceleration, and idling that are directly associated with vehicular emissions. The problem is that two very different driving cycles (e.g., one with many short stops, another with few long stops) may have the same average speed. A macroscopic emission model would provide the same emissions estimate when in fact the emission would be very different (Shabihkhani and Gonzales, 2014).

Intermediate mesoscopic emission models provide a compromise between the two extremes. The VT-Meso model, for example, uses link-by-link average speed, the number of vehicle stops, and stopped vehicle delay as aggregate traffic parameters to synthesize more detailed driving cycles that can be linked to the VT-micro emissions model (Rakha et al., 2011; Yue, 2008). Mesoscopic models have exploited the computational efficiency of aggregated traffic models and the accuracy of microscopic emissions models. There is no consensus on which model is the most accurate, in part because there have been relatively few studies comparing them (Hajmohammadi et al., 2019; Shorshani et al., 2015; Smit et al., 2010). An ongoing challenge is to determine an appropriate benchmark for network-wide emissions models because direct measurements across all vehicles in a network have not been available.

Efforts to identify systematic relationships between traffic models and emissions have started with analyses on traffic flow at signalized intersections (Shabihkhani and Gonzales, 2014; Skabardonis et al., 2013). At the network level, the MFD demonstrates

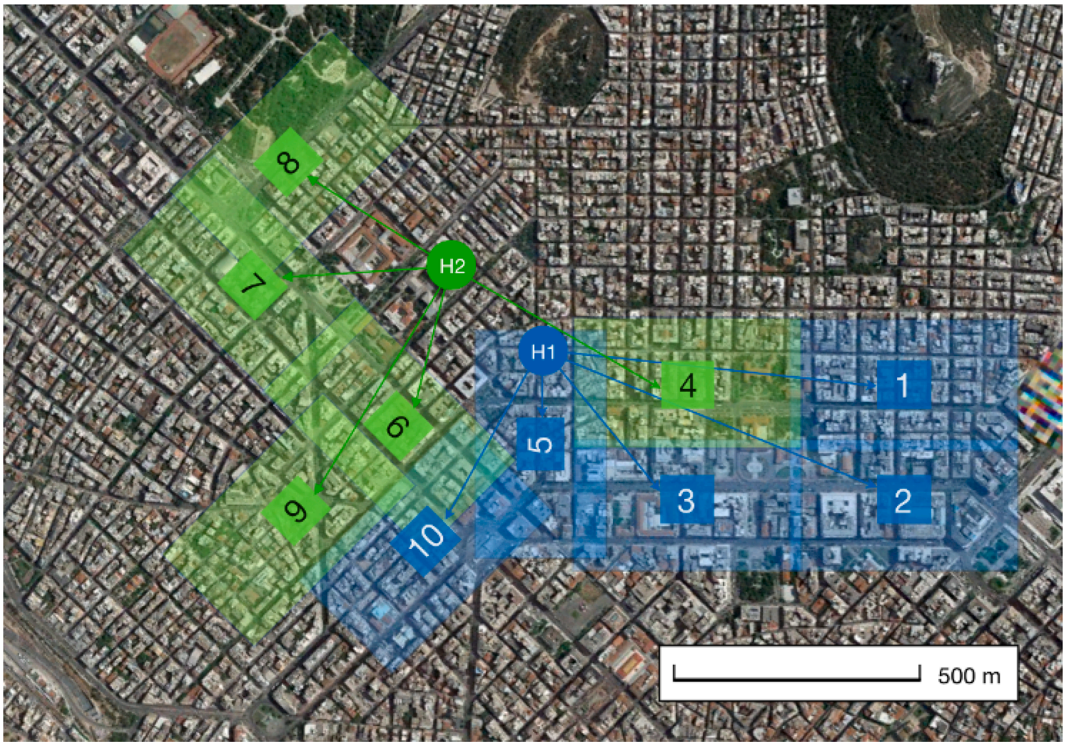

Fig. 1. Study area of pNEUMA experiment, and sub-areas assigned to each drone (Barmpounakis and Geroliminis, 2020).

consistent relationships between aggregated vehicle density, flow, and speed for many networks (Geroliminis and Daganzo, 2008). Shabihkhani and Gonzales (2014) noted that the theoretical underpinnings of the MFD suggest that consistent network-level relationships may also exist for driving cycle parameters that are most closely associated with emissions, namely the time that vehicles spend in the driving modes of cruising, idling, accelerating, and decelerating. The study showed that for idealized networks with uniform traffic conditions, the time spent cruising, time spent idling, and the number of vehicle stops are consistently related to vehicle density, like an MFD for emissions. Recently, Saedi et al. (2020) aimed at extending the scope to the urban network level with a simulation of Chicago.

Coupling traffic simulators with traffic emission models has been reported in the relevant literature as a good practice to estimate emissions in network level (Fontes et al., 2015; Osorio and Nanduri, 2015), or in a very recent study tailored for the city of Barcelona, Spain (Rodriguez-Rey et al., 2021). One of the biggest weaknesses of such efforts to model network-wide traffic emissions to date is the inability to validate models with real-world data due to its lack of availability. The pNEUMA dataset provides valuable comprehensive observations of vehicle trajectories within an urban network (Barmpounakis and Geroliminis, 2020). Trajectories that in the past could only be sampled or simulated are now directly observed for all vehicles with very high spatial and temporal resolution that allows microscopic emission models to be applied to every vehicle in the network.

It should be noted that due to the drawbacks of static and vehicle sensor networks for air quality monitoring (AQM), drones have also drawn the attention in this related research area (Hodgkinson et al., 2014). The idea of using UAS to collect more spatially sparse data is also reported in (Morawska et al., 2018), noting their main advantage against other methods to collect data in different altitudes. The lack of 3-dimensional data and the opportunities that rise with the use of UAS are also reported in (Yi et al., 2015). However, results from studies that deployed sensors on UAVs suggest that further improvements should be imposed to these kinds of sensors for the efficient and accurate collection of data (Alvarado et al., 2015). Thus, in the current study an alternative to calculating vehicles' emissions is proposed that takes advantage of the drones' ability to cover large areas and provide highly detailed data without the related caveats of installing sensors on them.

3. Methods

3.1. Data collection

In October 2018, the pNEUMA experiment was conducted in the city of Athens, Greece, aiming to record traffic streams over an urban setting using a swarm of ten drones (Barmpounakis and Geroliminis, 2020). The specific area was selected as an urban, multimodal, busy environment that can allow different kinds of transportation phenomena to be tested. The generalized scope of the pNEUMA experiment was to revolutionize how UAS as an emerging technology could reshape our understanding of traffic congestion

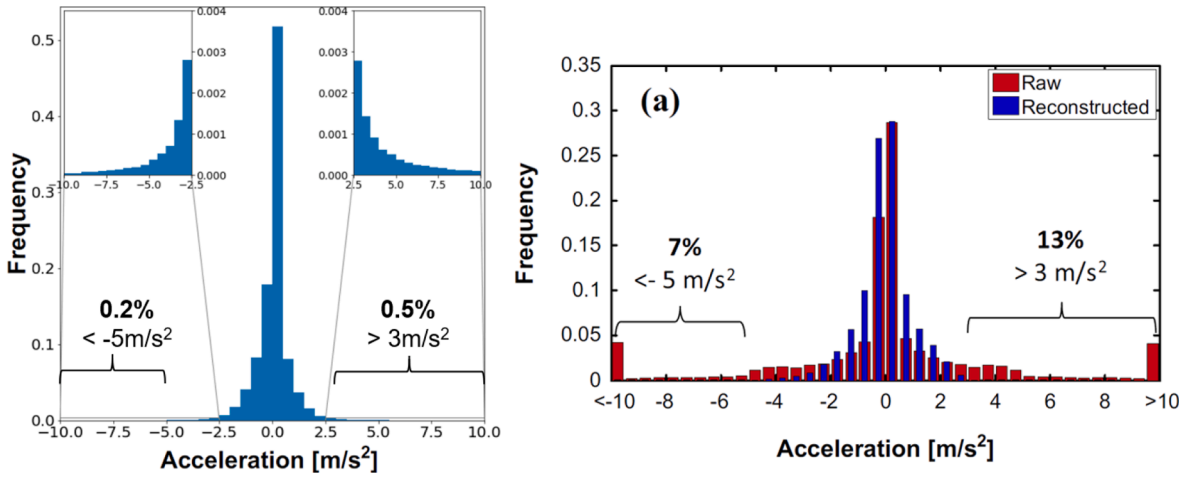

Fig. 2. pNEUMA acceleration frequency plot (left). NGSIM acceleration frequency plot (right) from (Montanino and Punzo, 2015).

mechanisms. Specifically, by putting the emphasis on urban networks with disturbances generated by interactions among different types of vehicles, the target was to better explain the mechanism of congestion formation and propagation in congested multimodal urban environments through massive data from aerial footage.

For the specific experiment, the morning peak (8:00–10:30) was recorded for each working day of a week. Specifically, the swarm would take-off from the two take-off/landing areas (H1 and H2 in Fig. 1) at the start of the experiment and each drone would go to its area of responsibility. Then, when all drones were at their hovering point, the recording of the traffic stream would start simultaneously and when the battery would run low, they would return to the landing point.

Considering that drones could hover up to 25 min including take-off, routing and landing times, it was decided that each session would take place every 30 min for better coordination and standardization of the experiment. This set-up allows 15–20 min of continuous monitoring of traffic, while during the temporal blind spots, trajectories were not recorded and were not related between sessions. The study area that was analyzed includes different types of arterials (low, medium and high-volume arterials), around 100 busy intersections (signalized or not), more than 60 bus stops and close to half a million observed vehicle trajectories.

A unique observatory for traffic congestion with data that did not exist before at this resolution and scale has been created from the processing of the videos from the experiment. This massive dataset contains trajectories of every vehicle that was present in the study area, calibrated in the WGS-84 system, every 0.04 s, as this is the maximum frequency allowed by the video's frame rate. Except for the features that can be produced using the position information, for example speed (first derivative of position), acceleration (second derivative of position), distance traveled etc., the type of each vehicle is available (car, taxi, motorcycle, bus, heavy vehicle, medium vehicle) is also available. More details on the design of the experiment can be found in (Barmpounakis and Geroliminis, 2020). Since the dataset is also part of an open science initiative shared to the research community, the data can be freely downloaded from https://open-traffic.epfl.ch.

3.2. Data accuracy

Empirical trajectories of all the vehicles in a network are the most precious data to investigate traffic dynamics and related phenomena. However, the accuracy of detailed trajectories has been a big concern, as measurements errors could corrupt vehicle dynamics and affect the reliability of related studies, especially for accelerations that are crucial for emission estimation. Punzo et al. (Punzo et al., 2011) unveiled significant measurement errors in NGSIM datasets, which was a major innovation in terms of trajectory data when it was created more than 10 years ago and has been widely used in the traffic research community. Many studies have made direct use of such data without considering the implications of measurement errors; others have applied off-the-shelf filtering/smoothing techniques (e.g., Savityky-Golay filter, low-pass filter, Kalman filter, moving average, and spline smoothing, among others). The main challenge of the latter methods is to remove noise while preserving underlying patterns of real driving behavior.

Our approach to assess the adequacy of pNEUMA data for microscopic emission modelling was to inspect and quantify their trajectory data accuracy following the methodology proposed in Montanino and Punzo (2015) and (Punzo et al., 2011). Physical, platoon, and internal consistency are all inspected. The former criterion analyzes the distribution of motion-related quantities to ensure that they fall within the normal physical limits. For acceleration, values should be between $-5 m/s^2$ and $3 m/s^2$ (illustrated in Fig. 2). When 1 s data resolution is examined, the analysis of speed and acceleration distributions shows great accuracy for the pNEUMA dataset. The outliers are below 1% of total observations, and they are not all necessarily errors as some harsh accelerations may occur in urban traffic, where aggressive drivers are not rare. Additionally, the internal consistency is preserved by how trajectories are obtained, and the inter-vehicle spacing analysis does not suggest platoon inconsistencies.

Fig. 2 illustrates the remarkable increase in accuracy that pNEUMA data signifies versus NGSIM data, the previous standard for empirical trajectory datasets. Both datasets were processed with light filtering techniques: spatial Kalman filter for pNEUMA, and

Table 1
Filtered pNEUMA dataset. Trajectories summary by vehicle type.

Vehicle Type	# of Trajectories
Bus	2663
Car	52,765
Heavy Vehicle	1396
Medium Vehicle	5340
Motorcycle	40,924
Taxi	20,805
Total	**123,893**

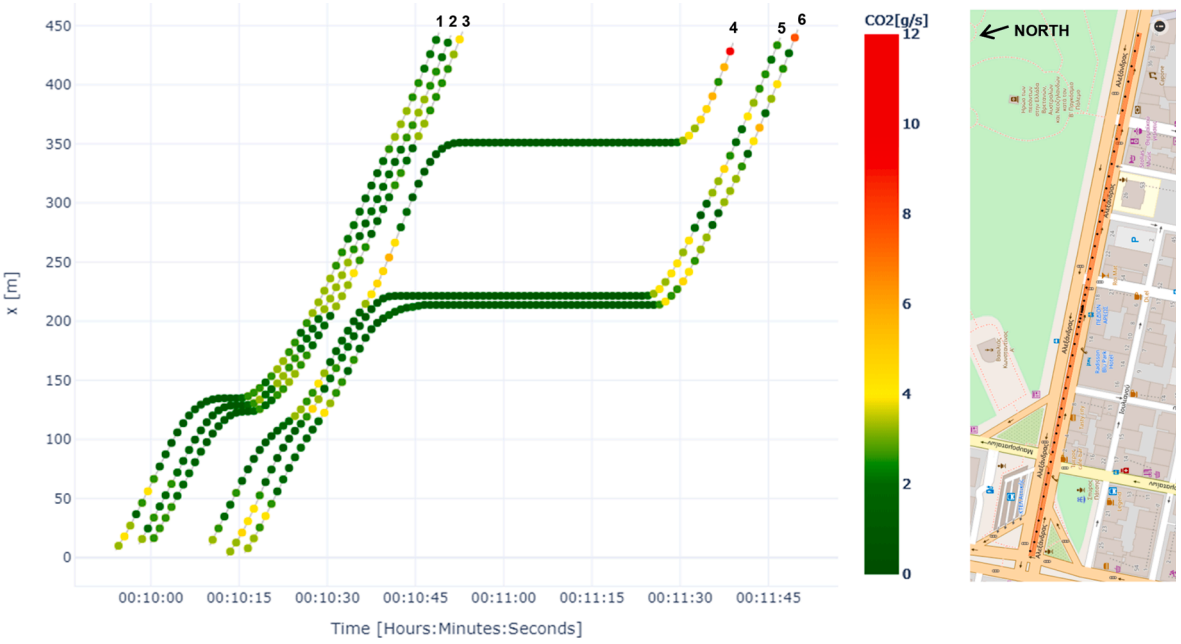

Fig. 3. Space-Time diagram with emission rates of 6 consecutive cars (left). Location: left lane of Alexandras Ave towards the East (right).

locally weighted regression for NGSIM. As a final remark, the NGSIM data frequency is lower (every 0.10 s), which reduces the number of extreme acceleration values.

3.3. Microscopic emission model

In this study, the project level of MOVES has been implemented to provide second-by-second emission estimates for each vehicle. MOVES is the official on-road emission model for the United States Environmental Protection Agency, and it was selected for this study because it is widely used in research and in practice. The MOVES microscopic model is based on the vehicle's specific power (VSP), a measure of the power demand based on the operating conditions. To compute it, it requires speed-acceleration profiles at 1 Hz. Additional inputs are vehicle type, year, fuel specification, road grade, and environmental conditions.

The vehicle type for MOVES, known as source type, is obtained by matching the vehicle type labels in the pNEUMA dataset with the corresponding MOVES vehicle categories. The age variable accounts for the fleet modernization effect; newer vehicles pollute less than older ones (all else being equal, MOVES estimates that emissions rates for a new car are around 30% lower than for a 10-year one). The average age of the fleet per vehicle type is derived from the European Automobile Manufacturers Association (2019), with all necessary adjustments based on the proportion of the vehicle fleet in pNEUMA dataset. Note that registration data is often used to infer the in-use vehicle fleet assuming it does not vary from the on-road fleet. However, Symeonidis et al. (2003) show that newer vehicles also tend to travel more kilometers, and thus, using registration data only leads to overestimating the fleet age.

Road grade also affects the power demand, as the engine must either work to overcome gravity (when traveling uphill) or is assisted by it (when traveling downhill). In the central district of Athens, slopes can reach up to 15%, which has a significant impact on emissions. The road grade information was derived from the STRM digital elevation model (Rabus et al., 2003). Environmental conditions inputs were held constant over all days of study, for a better comparability of the effect of different traffic characteristics on vehicular emissions. The assumed values are representative of the meteorological conditions in Athens when the experiment took

Table 2
Emissions summary by vehicle type, per trajectory.

	Average speed [km/h]	Average distance [m]	Average emissions per time traveled [g/s]	Average emissions per distance traveled [g/m]
Bus				
Mean	12.87	576.05	6.87	2.08
Std. deviation	5.25	263.14	1.87	0.56
Heavy Vehicle				
Mean	12.45	489.35	5.69	1.95
Std. deviation	6.83	208.41	1.61	0.72
Medium Vehicle				
Mean	14.61	528.15	1.84	0.55
Std. deviation	7.65	239.58	0.39	0.24
Car				
Mean	16.72	587.35	1.93	0.49
Std. deviation	7.86	280.62	0.40	0.19
Taxi				
Mean	16.05	585.88	2.05	0.53
Std. deviation	7.47	279.04	0.46	0.19
Motorcycle				
Mean	24.11	590.93	1.74	0.28
Std. deviation	9.60	276.21	0.49	0.06

place, with a temperature of 75°F (24 °C), and 70% humidity.

4. Results

The emissions we focus on our study are greenhouse gases (measured in units of CO_2 equivalent), because they are global pollutants that are most important to estimate in aggregate for a network. Note that these analyses can be extended to any other pollutant that can be estimated with a microscopic emissions model; e.g., MOVES provides estimates of many pollutants, including total hydrocarbons (THC), carbon monoxide (CO), nitrogen oxides (NO_X), sulfur dioxide (SO_2), particulate matter ($PM_{2.5}$ and PM_{10}), etc. (EPA US, 2012).

The results shown in the following subsections have been obtained after filtering the pNEUMA dataset to remove instances that add noise to the analysis of aggregated emission relationships with network traffic parameters. The filtering step removes parked vehicles, building occlusions, intervals where not all drones were recording, and areas with predominantly minor roads (as there, traffic dynamics are not influenced by other vehicles due to low accumulation). The resulting data subset is described in Table 1.

4.1. Emissions at the scale of individual vehicles

In this section, we first show the emissions produced along vehicle trajectories. It highlights the importance in emission estimation of accurate second-by-second speed-acceleration information, as well as the impact of driver behavior.

Fig. 3 provides an example to illustrate the emission rate per time along vehicle trajectories. The emission rate varies due to changes in speed and acceleration related to vehicle interactions with each other and traffic signal phasing. The highest emission rates per time traveled are associated with accelerations, either after idling at an intersection or to cross it just before the traffic signal turns red. A characteristic example of the latter can be seen in the 4th vehicle (counting from the left) where the CO_2 emissions are increased right before the 5th and 6th vehicles stop at the traffic signal (x = 225 m). Then the same vehicle must stop at the following traffic signal (x = 350 m). After the red phase, it is seen that the 4th vehicle, which has not gained a significant advantage over the 5th and 6th vehicle, also produces increased emissions compared to other vehicles. The above provide a first indication on how aggressive driving with high accelerations can be related to an increased ecological footprint without a significant advantage in reducing travel time. Finally, the trajectories show that accelerating at lower speeds is associated with lower emission rates compared to accelerating at higher speeds.

The data show that there is significant variability among trajectories, which results in the different levels of emissions generated by each vehicle. Averages of speed, emissions per time traveled and emissions per distance traveled are computed for each trajectory. Then, they are analyzed by vehicle type to reveal important differences within and between types in Table 2 (excluding trajectories shorter than 250 m). As expected, buses and heavy vehicles have the highest emission rates; with emissions per time traveled around 3 times higher than light vehicles, and almost 4 times higher for emissions per distance traveled. Nevertheless, if we consider that the average occupancy of passengers in buses in the study area during the peak period studied is in the range of 20 passengers per bus, then the emissions per bus passenger are 5–10 times smaller than for car passengers. There are small differences among cars, taxis, and medium vehicles, which are mainly caused by different driving patterns among vehicle types and different fuel types (diesel for taxis, and gasoline for cars and medium vehicles). Within the same vehicle type, there is also heterogeneity as indicated by the standard deviation values. Different traffic conditions, driving behaviors, and route choices in a hierarchical road network, among others, can cause large variations in emissions produced by identical vehicles. Finally, motorcycles present a more aggressive style of driving, which leads to relatively high emissions per time traveled, but they also travel at relatively high speeds for an urban network, keeping the emissions per distance traveled low.

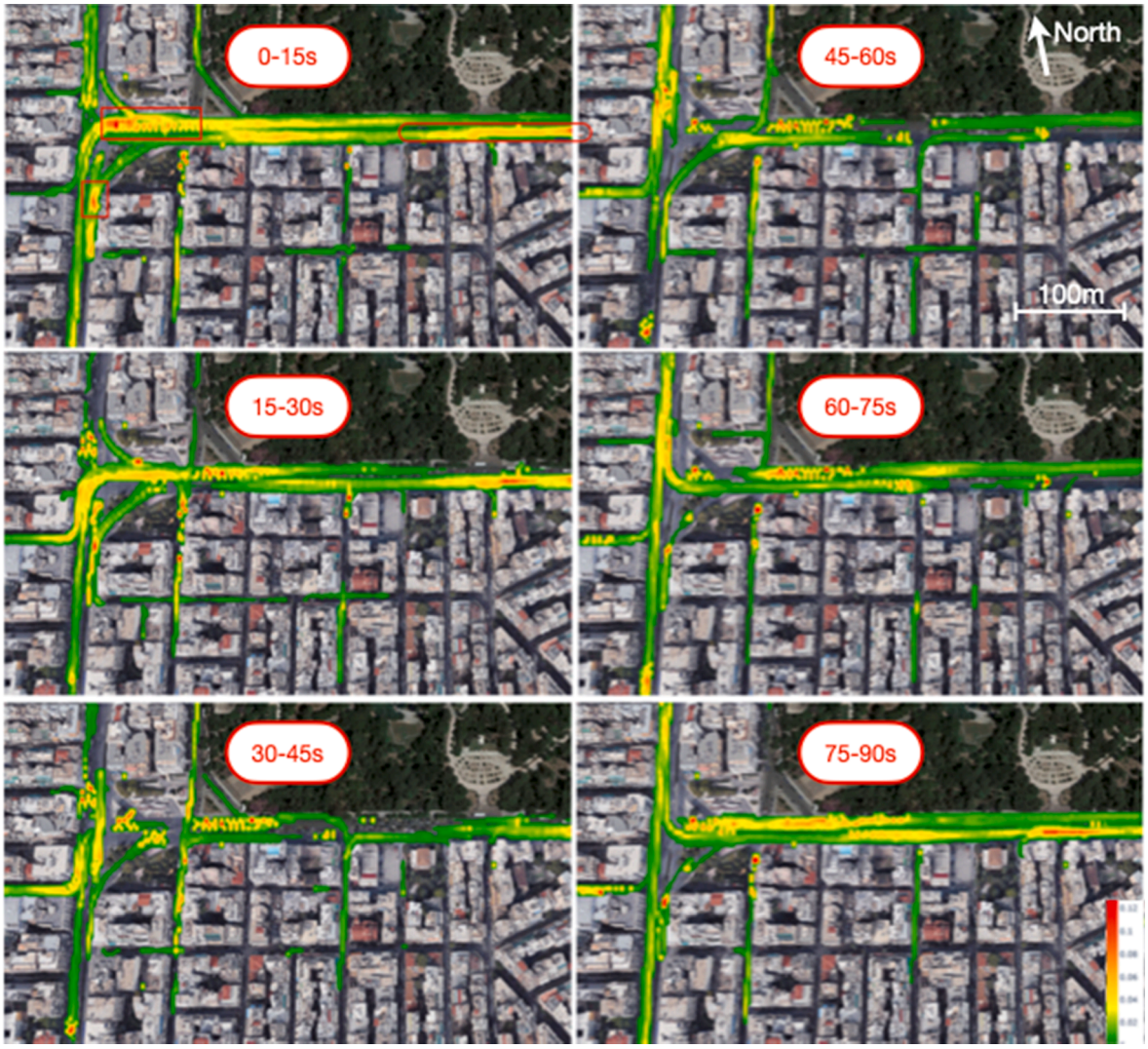

Fig. 4. Emissions density map (low in green; high in red) with 15 s aggregation for a 90 s signal cycle.

4.2. *Spatio-temporal distribution of emissions*

We show the relationship between emissions and traffic signal timing in Fig. 4. It illustrates the emission density in zone 8 (according to Fig. 1), aggregating the emissions of all vehicles in 15 s interval. The six images describe the spatiotemporal evolution of emissions over a signal cycle (90 s). In Fig. 4 (0–15 s), the high emission areas correspond to two queues of vehicles on the West side (in red rectangles); idling vehicles produce low emissions per vehicle-second but in total the emissions are high due to the high vehicle density. The temporal evolution follows with Fig. 4 (15–30 s), where the large queue discharges. It is worth mentioning that the high emission area observed in the East side (in a red oval) does not correspond to a high vehicle density area, but to a section of Alexandras Ave. with steep uphill grade for eastbound traffic.

The high emission areas are consistently near the most congested intersections. However, the most congested intersections vary over time, as shown in Fig. 5. The vehicle density and emissions increase from 8:00 to 10:00 AM. To compute emissions and vehicle density, we divide the roads into segments. For each resulting bin (approximately 20 m^2), we compute the total emissions produced over a time period (15 min) and average them. Hence, emissions are expressed per unit of time and per unit of area [$gCO_2/s/m^2$]. We proceed analogously for the vehicle density.

Finally, we study how concentrated the emissions are in the central district of Athens. Fig. 6 explains how much of the total emissions are produced in the most congested areas, and how much of the total congestion they account for. The congestion rank for the road segments is based on the normalized accumulation, and it is obtained by dividing the accumulation by the number of bins of each cluster. It should be noted that while normalized accumulation is conceptually close to density, it is slightly different as the bin area does not correspond exactly to the area of roads, because it is calculated based on the WGS-84 coordinates. Every data point

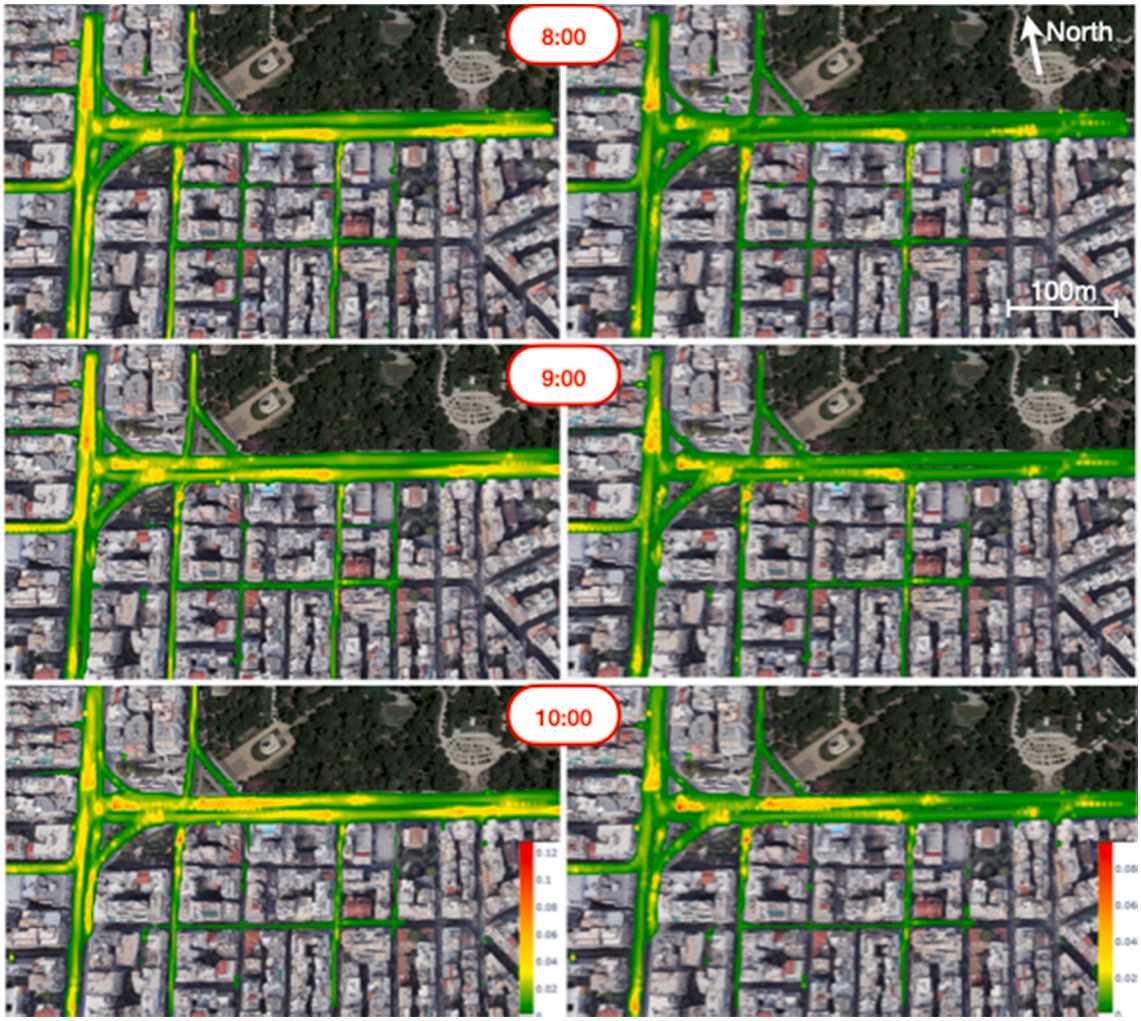

Fig. 5. Emissions density [$gCO_2/s/m^2$] (left) and Vehicle density [$veh/s/m^2$] (right) maps; with 15 min time intervals.

represents a time interval with the duration of a traffic signal cycle (90 s). The 20% most congested road segments (higher normalized accumulation) are responsible for 60% of the total congestion but only 50% of the total emissions. It can be interpreted as that a few emission hotspots are responsible for most of the vehicular pollution generated vehicles in an urban area. This highlights that advanced traffic management techniques, which could reduce the level of congestion in critical intersections through perimeter control (e.g., Kouvelas et al., 2017; Sirmatel and Geroliminis, 2021) or queue balancing (e.g., (Mercader et al., 2020; Varaiya, 2013), network emissions could be significantly reduced.

4.3. Macroscopic relationships in emissions

This section explores the existence of an emissions-MFD (e-MFD) from an experimental standpoint. Several analytical and micro-simulation works have already suggested that a reproducible relationship between aggregate emissions and vehicle accumulation in a network should exist, but the question remains if this is observed in the real world. To answer this question, we first perform spatial clustering, based on the total vehicular accumulation over the period of study, obtaining 10 static clusters of different size with equal accumulation. As previously introduced, the zones with lower density are filtered out, because they correspond to areas where traffic dynamics are not influenced by other vehicles, and the main effect is driver heterogeneity rather than congestion (e.g., in minor roads). This leaves 6 clusters for analysis.

Fig. 7 suggests that there is a well-defined speed MFD for the central district of Athens, and thus, it is worth exploring if there are also well-defined emissions network-level relationships. In the figure, 6 clusters (number 1 having the highest vehicular density) are plotted with normalized accumulation to account for the different surface area of each cluster. Each data point, obtained with the same procedure as described in the previous section, represents a 60 s-time interval (such time aggregation is used in every graph from now on).

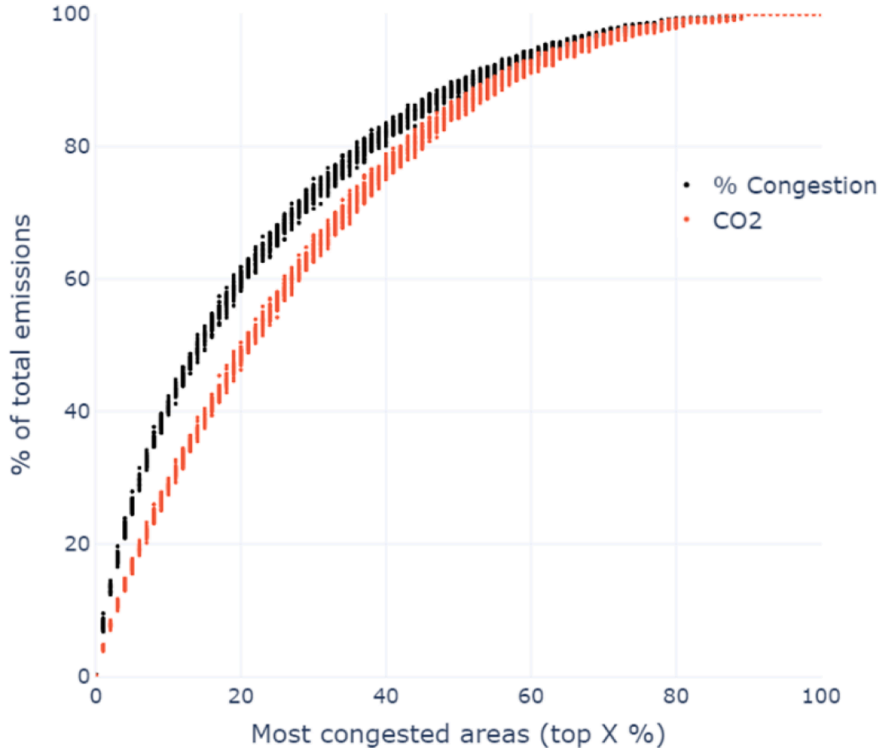

Fig. 6. Emissions distribution (bottom curve, red) and Congestion distribution (top curve, black).

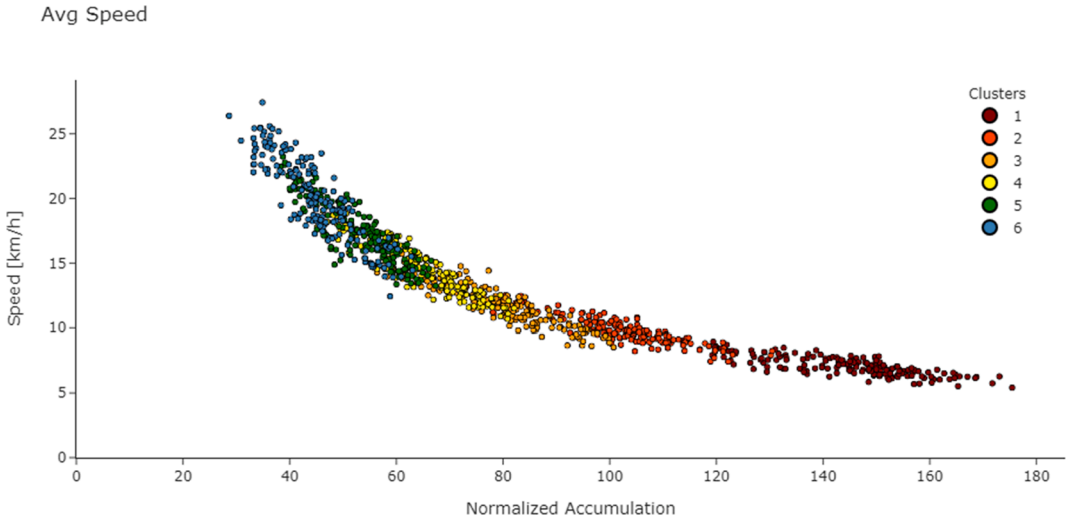

Fig. 7. Speed Macroscopic Fundamental Diagram (MFD).

Next, we investigate the aggregated relationships between emissions and average speed. Fig. 8 suggests that there is a well-defined e-MFD. Specifically, Fig. 8a shows that emissions per time travelled (measured in gCO_2 per vehicle-second) increases with average speed, which is due to the fact that vehicles spend more time moving (with higher emission rates) than idling (with low emission rate). Fig. 8b shows that the emissions per distance traveled (measured in grams of CO_2 per vehicle-meter) increase when average speed decreases. This happens because more congested traffic states require vehicles to spend more time traversing the same distance, and the effect of increased travel time is greater than any emissions reductions per unit time.

Combining the information from the figures above, a clearer illustration of a well-defined 3D e-MFD can be seen in Fig. 9. Compared to the 3D e-MFD reported in Saedi et al. (2020) for an aggregated measure of total emissions per time, the empirical e-MFD does not experience a hysteresis loop as the simulated one. A possible explanation might be that the size of hysteresis in the e-MFD might

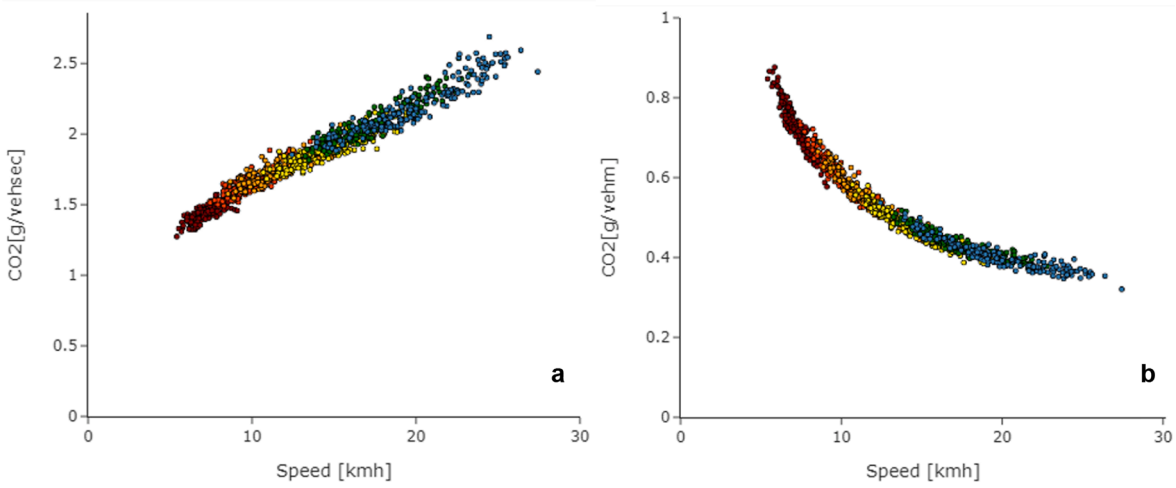

Fig. 8. Aggregated emissions per time traveled versus speed (a). Aggregated emissions per distance travelled versus speed (b).

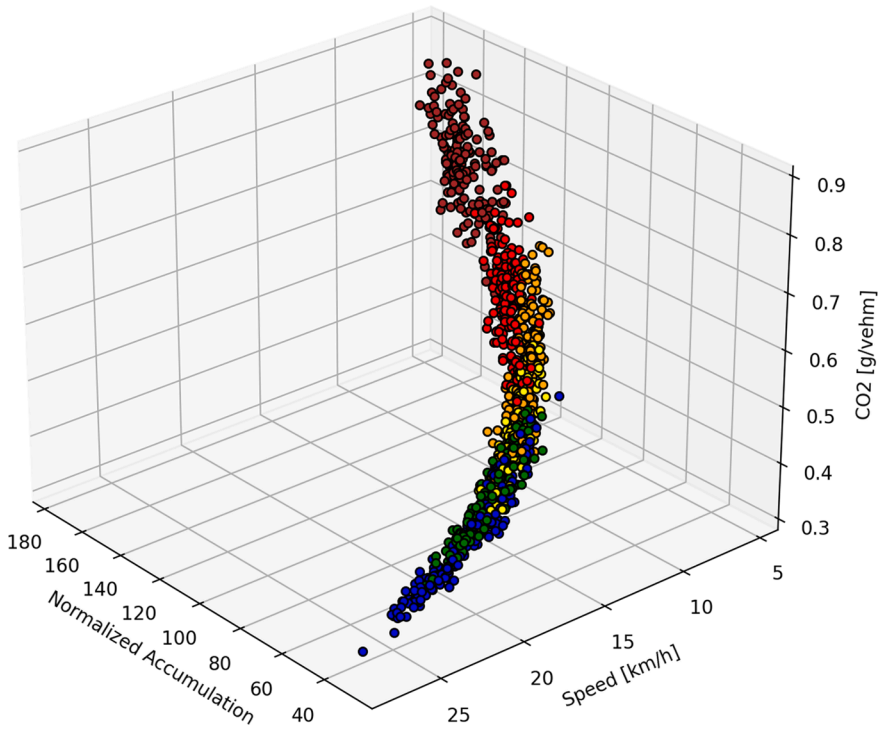

Fig. 9. 3D e-MFD illustrating accumulation versus speed versus aggregated emissions per distance travelled.

depend (similarly to the MFD) on the spatial distribution of congestion, the driver adaptability and the unloading demand profile (see for example (Mahmassani et al., 2013; Ramezani et al., 2015)). In principle, most simulation models are calibrated for the onset of congestion and the demand decreases quite sharply in the offset creating a higher hysteresis loop.

We would also like to highlight that while we present an aggregated macroscopic emission curve, this is based on emissions calculated on detailed trajectories of vehicles. Thus, these curves should not be considered universal, but clearly depend on the topology of the network and the signal control. There is clearly some similarity between aspects that affect the shape of an MFD (link length, signal settings, signal offsets, spatial distribution of congestion-see for example (Geroliminis and Boyaci, 2012) and (Dakic et al., 2020)) and the shape of an e-MFD. Nevertheless, emissions are significantly influenced by local congestion phenomena (stop-and-go traffic) that are correlated with space-mean speed and density but require additional investigation. A further analysis will clearly shed more light in this direction.

Vehicle emissions are determined by the driving cycles of the vehicles in the network, and this is reflected in the microscopic

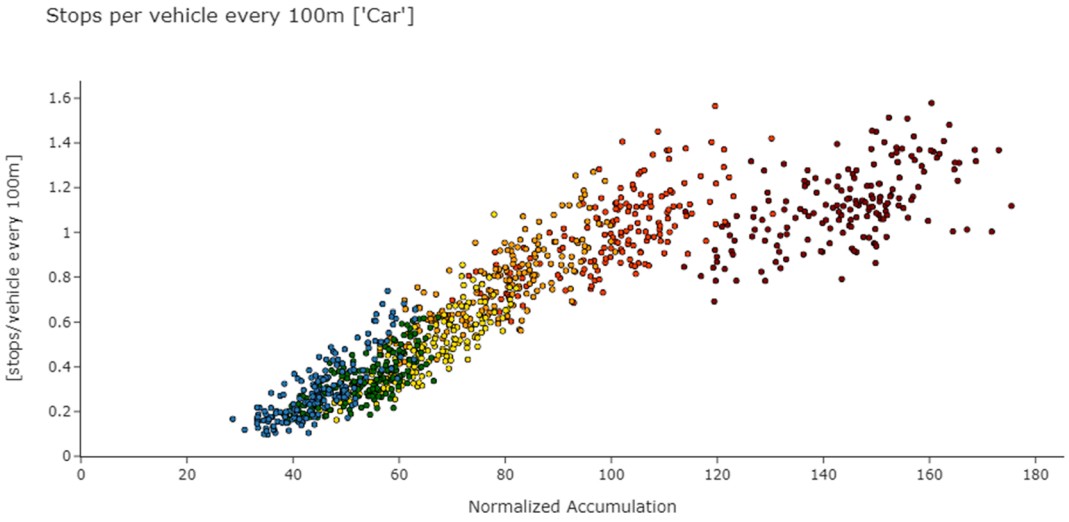

Fig. 10. Aggregated number of stops per vehicle-distance traveled as a function of normalized accumulation (only cars included).

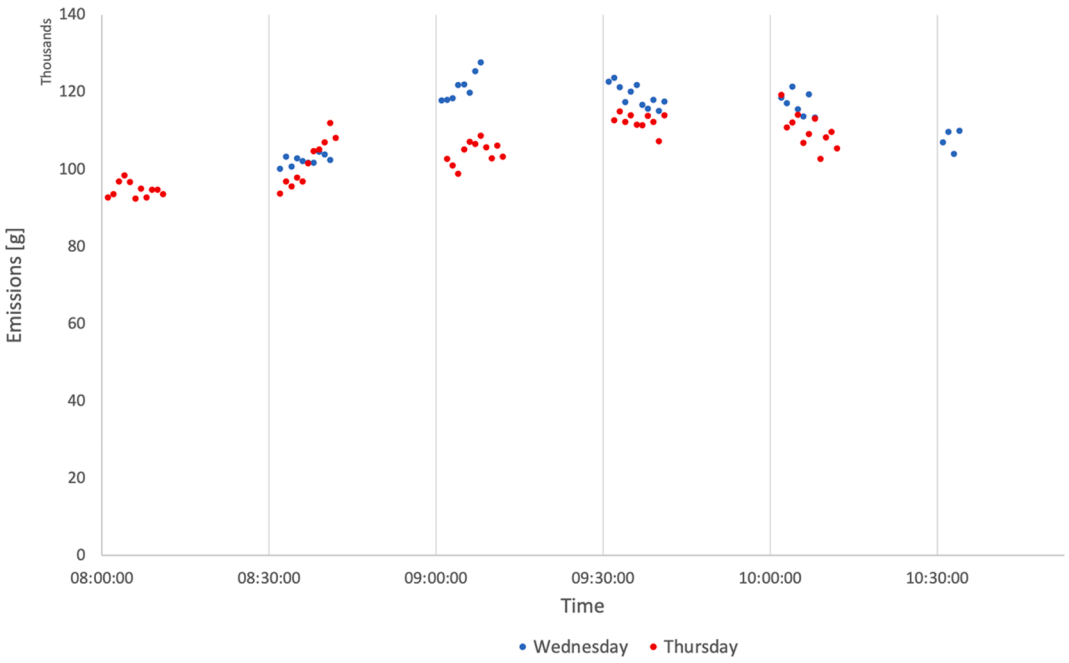

Fig. 11. Emissions variations between two different days.

emission models that relate vehicle second-by-second speed and acceleration to emission rates. In addition to the time it takes to traverse distance while cruising, traffic congestion is associated with more wasted time spent idling, which is reflected in lower average speed and excess emissions associated with idling. Vehicle accelerations are associated with the highest emission rates, and the time spent in acceleration is related to the number of times that each vehicle most stop while traversing distance. Fig. 10 shows how the number of vehicle stops per distance increases with congestion (higher normalized accumulation). To simplify the analysis and avoid the noise that non-congestion related stops could add (e.g., a taxi that stops to pick up a passenger), only cars are included. The consistent increase in stops per vehicle distance contributes to increased time in acceleration, which further contributes to increased emissions per distance with lower average speeds. It is important to understand that congestion increases total emissions (higher emissions for the same trip length), even though the average emission rate per time for a vehicle can be lower.

The data also shows that emissions can vary significantly between different days for the same network. In Fig. 11, the red markers show how emissions evolve during a normal working day in the study area, while with the blue markers show the evolution of emissions during another working day that a strike took place at 11:00 and thus led to increased vehicle accumulations earlier than

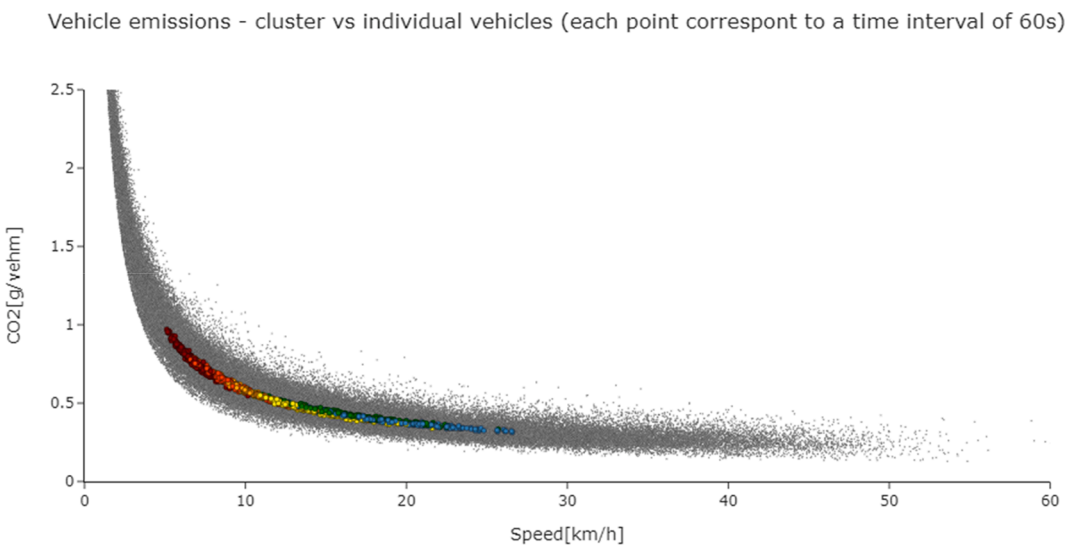

Fig. 12. Comparison of macroscopic level (clusters color code) and individual vehicle emissions (grey). Emissions measured in grams of CO_2 per vehicle-meter traveled (only cars included).

Table 3
Comparison of macroscopic level and individual vehicle emissions (only cars)

Speed [km/h]	Macroscopic level Emissions [g CO_2/veh-m]			Individual vehicle Emissions [g CO_2/veh-m]		
	Mean	Standard Deviation	Coefficient of Variation	Mean	Standard Deviation	Coefficient of Variation
[5.0, 7.5)	0.797	0.059	0.074	0.848	0.124	0.146
[7.5, 10.0)	0.644	0.042	0.064	0.658	0.095	0.145
[10.0, 12.5)	0.534	0.027	0.050	0.551	0.078	0.142
[12.5, 15.0)	0.467	0.018	0.039	0.486	0.068	0.141
[15.0, 17.5)	0.421	0.015	0.036	0.438	0.063	0.144
[17.5, 20.0)	0.389	0.012	0.031	0.401	0.061	0.152
[20.0, 22.5)	0.363	0.010	0.028	0.370	0.058	0.157

normal. Note that even if an aggregated relation between network speed and emissions is shown, these emissions have been calculated with a detailed emission model that utilizes individual vehicle trajectory data, detailed acceleration measures, and topological information. If instead, someone used a simple emission model that considers only the average vehicles' speed or a model that considers the vehicles' operation modes (idle, acceleration, deceleration, cruise), the total emissions would be underestimated up to 30% for specific types of vehicles with big errors in estimation for individual vehicles. Specifically, by using the adjusted curve $y = C\left[891 - 22.1360x + 0.2346x^2 - 0.0007x^3\right]$, where y is the CO_2 emission rate in g/km, x is the average speed in km/h and C = 0.55 (correction factor), the underestimated emissions for heavy vehicles is 86% and for cars and taxis is 27% while motorcycles are overestimated by 46%. Thus, the e-MFD shows more consistent relationships at the aggregate level.

Finally, we add a note on the importance of macroscopic modeling of emissions. Fig. 12 shows that there is a well-defined relationship between emissions and speed at macroscopic level, while at individual level (single vehicle) there is higher variance and one can observe heteroskedasticity. The same 6 clusters based on vehicular density are illustrated in color while the data for individual cars are shown in gray. Although the variability among individual cars makes the emissions from any single vehicle difficult to accurately estimate, the aggregated emissions across the network are much more consistent. Table 3 summarizes the same data, with standard deviation and coefficient of variation as measures of dispersion presented for both the aggregated macroscopic level and individual microscopic level.

5. Conclusions

This paper focuses on analyzing the vehicle emissions in a multimodal urban network by utilizing massive trajectory data from a swarm of drones. It has an unprecedented scope, due to the large area covered with detailed trajectories combined with microscopic emission modelling, which is deemed necessary to provide appropriate insight into the underlying mechanisms of vehicular emissions. This offers a unique opportunity to investigate disaggregated and aggregated relations between emissions and congestion patterns.

The results show the impact of traffic related stops on emissions, with high emission levels near intersections. The dynamics of emissions are illustrated with emission density maps and their evolution over time. The spatial distribution of congestion and

emissions is analyzed, quantifying the contribution to the total emissions of the most congested areas in the network.

A well-defined e-MFD is observed and the macroscopic relationships between aggregated traffic variables and emission metrics are further discussed. With more congestion, the total emissions increase, due to the scaling effect of having more vehicles in the network but also because the unit emissions per vehicle-distance traveled increase as well. The empirical results are consistent with theoretical and simulated relationships presented in (Shabihkhani and Gonzales, 2014). The number vehicle stops per distance travelled, which corresponds to the cycles of deceleration and acceleration that are important determinants of vehicle emissions, increases approximately linearly with vehicle accumulation as expected from traffic flow theory. The theory and simulations predict that emissions per vehicle distance traveled increase as an increasing exponential function of speed, which is consistent with the empirical results that show emissions per distance traveled decreasing exponentially with speed, and speed decreasing exponentially with vehicle accumulation. The difference is that the empirical data in this paper are specific to the real Athens network rather than an idealized, uniform, grid network. More research in a broad range of congestion levels and network topologies would be beneficial to better understand these relationships.

Additionally, the results show empirical evidence of the differences among vehicle types regarding emissions produced, which is not only caused by their technical specifications but also by driving behaviors. This vast information about emissions in real driving conditions can be used by cities to derive policies targeting those types of vehicles or aggressive drivers that contribute more to the emissions footprint. In this spirit, simple strategies are already being used in low emission zones to reduce the city's emission footprint by limiting the use of high pollutant vehicles (e.g., diesel heavy vehicles). By relating aggregate traffic dynamics to emissions, the e-MFD provides a mechanism to link network-wide traffic control and demand management policies to emissions reduction objectives.

The specific study can be extended by comparing different microscopic models for calculating emissions, exploring their differences and seeing how and if the form of the e-MFD varies. The study can also become a benchmark to perform original research related to network traffic and emissions.

Declaration of Competing Interest

The authors declare that they have no known competing financial interests or personal relationships that could have appeared to influence the work reported in this paper.

Acknowledgments

This research was partially funded by Swiss National Science Foundation (grant no. 200021_188590) "pNEUMA: On the new era of urban traffic models with massive empirical data from aerial footage.''

Data Source: pNEUMA – open-traffic.epfl.ch.

Author contributions

All authors contributed to all aspects of the study, reviewed the results and approved the final versions of the manuscript.

References

Agency, U.E.P., 2003. User's guide to MOBILE6 1 and MOBILE6. 2 Mobile Source Emission Factor Model.

Alson, J., Hula, A., Bunker, A., 2014. Light-duty automotive technology, carbon dioxide emissions, and fuel economy trends: 1975 through 2013 - executive summary, in: Fuel Economy: Standards, Trends, and Technological Developments.

Alvarado, M., Gonzalez, F., Fletcher, A., Doshi, A., 2015. Towards the development of a low cost airborne sensing system to monitor dust particles after blasting at open-pit mine sites. Sensors (Switzerland) 15 (8), 19667–19687. https://doi.org/10.3390/s150819667.

Avl cruise – vehicle system and driveline analysis [WWW Document], 2017. URL https://www.avl.com/cruise.

Barmpounakis, E., Geroliminis, N., 2020. On the new era of urban traffic monitoring with massive drone data: The pNEUMA large-scale field experiment. Transp. Res. Part C Emerg. Technol. 111, 50–71. https://doi.org/10.1016/j.trc.2019.11.023.

Barth, M., An, F., Younglove, T., Scora, G., Levine, C., Ross, M., Wenzel, T., 2000. Development of a Comprehensive Modal Emissions Model. Natl. Coop. Highw. Res. Program, Web-Only Doc., p. 122

CARB, 2015. EMFAC2014 Volume III – Technical Documentation.

Dakic, I., Ambühl, L., Schümperlin, O., Menendez, M., 2020. On the modeling of passenger mobility for stochastic bi-modal urban corridors. Transp. Res. Part C Emerg. Technol. 113, 146–163. https://doi.org/10.1016/j.trc.2019.05.018.

EMFAC2007, 2007. Calculating Emission Inventories for Vehicles in California. Calif. Air Resour. Board, Sacramento.

EPA US, 2012. Motor Vehicle Emission Simulator (MOVES): User guide for MOVES 2010b.

European Automobile Manufacturers Association, 2019. Vehicles in use Europe, 2019.

Fontes, T., Pereira, S.R., Fernandes, P., Bandeira, J.M., Coelho, M.C., 2015. How to combine different microsimulation tools to assess the environmental impacts of road traffic? Lessons and directions. Transp. Res. Part D Transp. Environ. 34, 293–306. https://doi.org/10.1016/j.trd.2014.11.012.

Frey, H.C., 2018. Trends in onroad transportation energy and emissions. J. Air Waste Manag. Assoc. 68 (6), 514–563. https://doi.org/10.1080/10962247.2018.1454357.

Frey, H.C., Zhang, K., Rouphail, N.M., 2008. Fuel use and emissions comparisons for alternative routes, time of day, road grade, and vehicles based on in-use measurements. Environ. Sci. Technol. 42 (7), 2483–2489.

Geroliminis, N., Boyacı, B., 2012. The effect of variability of urban systems characteristics in the network capacity. Transp. Res. Part B Methodol. 46 (10), 1607–1623. https://doi.org/10.1016/j.trb.2012.08.001.

Geroliminis, N., Daganzo, C.F., 2008. Existence of urban-scale macroscopic fundamental diagrams: Some experimental findings. Transp. Res. Part B Methodol. 42 (9), 759–770. https://doi.org/10.1016/j.trb.2008.02.002.

Hajmohammadi, H., Marra, G., Heydecker, B., 2019. Data-driven models for microscopic vehicle emissions. Transp. Res. Part D Transp. Environ. 76, 138–154. https://doi.org/10.1016/j.trd.2019.09.013.

Hausberger, S., 2003. Simulation of Real World Vehicle Exhaust Emission.
Hodgkinson, B., Lipinski, D., Peng, L., Mohseni, K., 2014. High resolution atmospheric sensing using UAVs, in: Springer Tracts in Advanced Robotics. https://doi.org/10.1007/978-3-642-55146-8_3.
Int Panis, L., Broekx, S., Liu, R., 2006. Modelling instantaneous traffic emission and the influence of traffic speed limits. Sci. Total Environ. 371 (1-3), 270–285. https://doi.org/10.1016/j.scitotenv.2006.08.017.
Keller, M., Hausberger, S., Matzer, C., Wüthrich, P., Notter, B., 2017. HBEFA Version 3.3. Backgr. Doc. Berne 12.
Kouvelas, A., Saeedmanesh, M., Geroliminis, N., 2017. Enhancing model-based feedback perimeter control with data-driven online adaptive optimization. Transp. Res. Part B Methodol. 96, 26–45. https://doi.org/10.1016/j.trb.2016.10.011.
Kumar Pathak, S., Sood, V., Singh, Y., Channiwala, S.A., 2016. Real world vehicle emissions: Their correlation with driving parameters. Transp. Res. Part D Transp. Environ. 44, 157–176. https://doi.org/10.1016/j.trd.2016.02.001.
Lejri, D., Can, A., Schiper, N., Leclercq, L., 2018. Accounting for traffic speed dynamics when calculating COPERT and PHEM pollutant emissions at the urban scale. Transp. Res. Part D Transp. Environ. 63, 588–603. https://doi.org/10.1016/j.trd.2018.06.023.
Mahmassani, H.S., Saberi, M., Zockaie, A., 2013. Urban network gridlock: Theory, characteristics, and dynamics. Transp. Res. Part C Emerg. Technol. 36, 480–497. https://doi.org/10.1016/j.trc.2013.07.002.
Mercader, P., Uwayid, W., Haddad, J., 2020. Max-pressure traffic controller based on travel times: An experimental analysis. Transp. Res. Part C Emerg. Technol. 110, 275–290.
Montanino, M., Punzo, V., 2015. Trajectory data reconstruction and simulation-based validation against macroscopic traffic patterns. Transp. Res. Part B Methodol. https://doi.org/10.1016/j.trb.2015.06.010.
Morawska, L., Thai, P.K., Liu, X., Asumadu-Sakyi, A., Ayoko, G., Bartonova, A., Bedini, A., Chai, F., Christensen, B., Dunbabin, M., Gao, J., Hagler, G.S.W., Jayaratne, R., Kumar, P., Lau, A.K.H., Louie, P.K.K., Mazaheri, M., Ning, Z., Motta, N., Mullins, B., Rahman, M.M., Ristovski, Z., Shafiei, M., Tjondronegoro, D., Westerdahl, D., Williams, R., 2018. Applications of low-cost sensing technologies for air quality monitoring and exposure assessment: How far have they gone? Environ. Int. 116, 286–299. https://doi.org/10.1016/j.envint.2018.04.018.
Ntziachristos, L., Gkatzoflias, D., Kouridis, C., Samaras, Z., 2009. COPERT: A European road transport emission inventory model. Environ. Sci. Eng. (Subseries Environ. Sci. https://doi.org/10.1007/978-3-540-88351-7-37.
Nyhan, M., Sobolevsky, S., Kang, C., Robinson, P., Corti, A., Szell, M., Streets, D., Lu, Z., Britter, R., Barrett, S.R.H., Ratti, C., 2016. Predicting vehicular emissions in high spatial resolution using pervasively measured transportation data and microscopic emissions model. Atmos. Environ. 140, 352–363. https://doi.org/10.1016/j.atmosenv.2016.06.018.
Osorio, C., Nanduri, K., 2015. Urban transportation emissions mitigation: Coupling high-resolution vehicular emissions and traffic models for traffic signal optimization. Transp. Res. Part B Methodol. 81, 520–538. https://doi.org/10.1016/j.trb.2014.12.007.
Perugu, H., 2019. Emission modelling of light-duty vehicles in India using the revamped VSP-based MOVES model: The case study of Hyderabad. Transp. Res. Part D Transp. Environ. 68, 150–163. https://doi.org/10.1016/j.trd.2018.01.031.
Punzo, V., Borzacchiello, M.T., Ciuffo, B., 2011. On the assessment of vehicle trajectory data accuracy and application to the Next Generation SIMulation (NGSIM) program data. Transp. Res. Part C Emerg. Technol. 19 (6), 1243–1262. https://doi.org/10.1016/j.trc.2010.12.007.
Rabus, B., Eineder, M., Roth, A., Bamler, R., 2003. The shuttle radar topography mission - A new class of digital elevation models acquired by spaceborne radar. ISPRS J. Photogramm. Remote Sens. https://doi.org/10.1016/S0924-2716(02)00124-7.
Rakha, H., Van Aerde, M., Ahn, K., Trani, A., 2000. Requirements for evaluating traffic signal control impacts on energy and emissions based on instantaneous speed and acceleration measurements. Transp. Res. Rec. 1738 (1), 56–67. https://doi.org/10.3141/1738-07.
Rakha, H., Yue, H., Dion, F., 2011. VT-Meso model framework for estimating hotstabilized light-duty vehicle fuel consumption and emission rates. Can. J. Civ. Eng. 38 (11), 1274–1286. https://doi.org/10.1139/l11-086.
Ramezani, M., Haddad, J., Geroliminis, N., 2015. Dynamics of heterogeneity in urban networks: Aggregated traffic modeling and hierarchical control. Transp. Res. Part B Methodol. 74, 1–19. https://doi.org/10.1016/j.trb.2014.12.010.
Rodriguez-Rey, D., Guevara, M., Linares, M.P., Casanovas, J., Salmerón, J., Soret, A., Jorba, O., Tena, C., Pérez García-Pando, C., 2021. A coupled macroscopic traffic and pollutant emission modelling system for Barcelona. Transp. Res. Part D Transp. Environ. 92, 102725. https://doi.org/10.1016/j.trd.2021.102725.
Saedi, R., Verma, R., Zockaie, A., Ghamami, M., Gates, T.J., 2020. Comparison of Support Vector and Non-Linear Regression Models for Estimating Large-Scale Vehicular Emissions, Incorporating Network-Wide Fundamental Diagram for Heterogeneous Vehicles. Transp. Res. Rec. https://doi.org/10.1177/0361198120914304.
Shabihkhani, R., Gonzales, E., 2014. Macroscopic relationship between network-wide traffic emissions and fundamental properties of the network, in: Transportation Research Circular E-C197. Proc., Symposium Celebrating. pp. 284–299.
Fallah Shorshani, M., André, M., Bonhomme, Céline, Seigneur, C., 2015. Modelling chain for the effect of road traffic on air and water quality: Techniques, current status and future prospects. Environ. Model. Softw. 64, 102–123.
Sirmatel, I.I., Geroliminis, N., 2021. Stabilization of city-scale road traffic networks via macroscopic fundamental diagram-based model predictive perimeter control. Control Eng. Pract. 109, 104750. https://doi.org/10.1016/j.conengprac.2021.104750.
Skabardonis, A., Geroliminis, N., Christofa, E., 2013. Prediction of vehicle activity for emissions estimation under oversaturated conditions along signalized arterials. J. Intell. Transp. Syst. 17 (3), 191–199.
Smit, R., Ntziachristos, L., Boulter, P., 2010. Validation of road vehicle and traffic emission models - A review and meta-analysis. Atmos. Environ. 44 (25), 2943–2953. https://doi.org/10.1016/j.atmosenv.2010.05.022.
Smit, R., Smokers, R., Rabé, E., 2007. A new modelling approach for road traffic emissions: VERSIT+. Transp. Res. Part D Transp. Environ. https://doi.org/10.1016/j.trd.2007.05.001.
Sun, Z., Hao, P., Ban, X. (Jeff) J., Yang, D., 2015. Trajectory-based vehicle energy/emissions estimation for signalized arterials using mobile sensing data. Transp. Res. Part D Transp. Environ. 34, 27–40. https://doi.org/10.1016/j.trd.2014.10.005.
Symeonidis, P., Ziomas, I., Proyou, A., 2003. Emissions of air pollutants from the road transport sector in Greece: Year to year variation and present situation. Environ. Technol. 24 (6), 719–726.
Varaiya, P., 2013. Max pressure control of a network of signalized intersections. Transp. Res. Part C Emerg. Technol. 36, 177–195.
Yi, W.Y., Lo, K.M., Mak, T., Leung, K.S., Leung, Y., Meng, M.L., 2015. A survey of wireless sensor network based air pollution monitoring systems. Sensors (Switzerland) 15, 31392–31427. https://doi.org/10.3390/s151229859.
Yue, H., 2008. Mesoscopic fuel consumption and emission modeling. Virginia Tech.